Microwave Resonance and Carrier-Carrier Interaction in Two-Dimensional Hole Systems at High Magnetic Field

C.-C. Li, J. Yoon, L. W. Engel†, D. Shahar*, D. C. Tsui, and M. Shayegan
Department of Electrical Engineering, Princeton University, Princeton, NJ 08544
†*National High Magnetic Field Laboratory, Florida State University, Tallahassee, FL 32306*
**Department of Condensed Matter Physics, Weizmann Institute, Rehovot 76100, Israel*

Microwave frequency conductivity, $\mathrm{Re}(\sigma_{xx})$, of high quality two-dimensional hole systems (2DHS) in a large perpendicular magnetic field (B) is measured with the carrier density (n_s) of the 2DHS controlled by a backgate bias. The high B insulating phase of the 2DHS exhibits a microwave resonance that remains well-defined, but shifts to higher peak frequency (f_{pk}) as n_s is reduced. Over a wide range of n_s, $f_{pk} \propto n_s^{-1/2}$ is observed for the two samples we measured. The data clearly indicate that both carrier-carrier interactions and disorder are indispensable in determining the dynamics of the insulator. The n_s dependence of f_{pk} is consistent with a weakly pinned Wigner crystal in which domain size increases with n_s, due to larger carrier-carrier interaction.

PACS numbers: 73.40Hm, 73.50Mx, 75.40Gb

In high magnetic field, B, sufficiently high quality two dimensional systems of electrons or holes (2DES or 2DHS) in semiconductors exhibit the fractional quantum Hall effect (FQHE) [1], a spectacular manifestation of carrier-carrier interaction. In the high B limit, samples that show the FQHE become insulators, and it is natural to ask what is the role of the carrier-carrier interaction in this insulating phase. The fields and carrier densities at which the high B insulating phase appears in FQHE-exhibiting samples are in rough agreement with predictions [2] of the appearance of a Wigner crystal (WC), stabilized by the freezing out of the kinetic energy in the magnetic field. In a WC ground state, carriers form a lattice, to minimize the energy of their mutual repulsion, so carrier-carrier interaction is of central importance. For a WC to be an insulator, disorder is required, which pins the WC, and also causes the WC to have finite correlation length, or domain size (L). On the other hand, if disorder is too strong, the carrier-impurity interaction can localize carriers resulting in an insulator without Wigner crystalline order. Hence the central questions about the high B insulating phases pertain to a competition between carrier-carrier and carrier-impurity interactions.

The picture of a pinned WC motivated many different types of experiments [3–13] on the high B insulator, including conduction [3–5], noise generation [3,4], giant dielectric constant [6], ac-dc interference [7], cyclotron resonance [8], and photoluminesence measurements [9]. Microwave measurements [5,10–13], such as those presented here, reveal resonant absorption in the high B insulators of samples capable of exhibiting the FQHE. Such resonances are typically interpreted as "pinning modes", in which WC domains oscillate within the pinning potential of the disorder.

Theories due to Fukuyama and Lee (FL) [14], and later investigators [15] describe the pinning mode as WC domains oscillating in parabolic restoring potentials. The potentials are proportional to ω_0^2, where ω_0 is called the pinning frequency. In the magnetic field, such oscillators have two modes. The higher mode frequency, ω_+, is shifted above the cyclotron frequency $\omega_c = eB/m^*$, where m^* is the carrier effective mass. If $\omega_0 \ll \omega_c$, the lower mode frequency, ω_-, is ω_0^2/ω_c, and is identified with $2\pi f_{pk}$, where f_{pk} is the measured resonance peak frequency. It is important to note that the m^* cancels in the expression for f_{pk}. In units of $\mathrm{Re}(\sigma_{xx})$ integrated over f, FL obtain oscillator strengths of $S = n_s \pi f_{pk} e/B$ for the lower mode. Recent measurements [12] on high quality 2DHS show resonances that depend on B in a way the FL theory cannot readily explain and that are too sharp to be explained easily as independently oscillating, disorder-induced domains. As yet, a real understanding of the static configuration of the insulator, as well as its dynamics, is lacking.

In this paper we directly address the centrally important competition between carrier-carrier and carrier-impurity interaction, by varying carrier density n_s in a sample, without warming it up. This effectively varies the carrier-carrier interactions while leaving the disorder potential unchanged. We present data on the microwave resonance of the high B insulating phase of high quality 2DHS samples, measured with varying hole density (n_s) by means of a dc bias voltage applied to a backgate. In a constant B of 13 T, the resonance peak remains well-defined, with decreasing peak height, as n_s is reduced. The evolution of the resonance peak with decreasing n_s shows a true shift of center frequency, f_{pk}, not just a lopsided f-dependent reduction of intensity. This change in oscillator center frequency must be due to carrier-carrier interaction, and we can reject any picture of the resonance with purely independent carriers. Interpretation of the decreasing f_{pk} vs n_s in terms of a pinned WC requires a "weak pinning" model, in which domain size L is determined by a balance between the carrier-carrier interaction and carrier-impurity interaction energies [14], and in which L increases with increasing n_s. Over a wide range in n_s, for the samples we examined, $f_{pk} \propto n_s^{-1/2}$, in agreement with theory [14,15] for fixed B.

The microwave technique for measurement of Re(σ_{xx}) was just as in refs. [11] and [12]. Re(σ_{xx}) was obtained from the attenuation of a microwave transmission line, patterned onto the top of the sample, as shown in the inset to Fig. 1, and coupled capacitively to the 2DHS. No spatial harmonics were observed, so the experiment is sensitive to σ_{xx} with wavevector $q \lesssim 2\pi/W$, where $W = 30$ μm is the width of gap between center and side conductors of the line. Hence we take the Re(σ_{xx}) data presented as characteristic of the 2DHS in the long wavelength limit. The real part of the diagonal conductivity is calculated from transmitted power P as in refs. [11,12], Re(σ_{xx})=$W|\ln P|/2Z_0 d$, where d=28 mm is the total length of the transmission line. $Z_0 = 50\Omega$ and is the transmission line characteristic impedance when $n_s = 0$, and P is normalized to unity for that condition. Errors of this formula are estimated as in refs. [11,12], as 15 percent, with the apparatus typically 20 times more sensitive to Re(σ_{xx}) than it is to Im(σ_{xx})

We present data on two p-type samples (1 and 2), from wafers also used by Santos *et al.* [16] in an observation of re-entrance of insulating behavior around the 1/3 FQHE. Sample 1 was from the same wafer used in an earlier microwave study [12] of the high B insulator. Samples 1 and 2 are both GaAs/Al_xGa_{1-x}As heterostructures grown on (311)A GaAs substrate, with Si modulation doping in two layers. The n_s of each sample was reduced by means of a bias voltage applied to a backgate, and measured at various positive backgate bias voltages from the quantum Hall effect. Increasing n_s with negative bias was impractical due to parallel conduction. At zero bias, sample 1 had $n_s \sim 5.5 \times 10^{10}$ cm^{-2}, and mobility 3.5×10^5 cm^2/V-s, while sample 2 had $n_s \sim 4.2 \times 10^{10}$ cm^{-2}, and mobility 5.0×10^5 cm^2/V-s. Details of the growth of the samples are similar; parameters of the nearest doping layer to the 2DHS may be relevant to the data we will present: sample 1 (sample 2) has 1150 Å (1200Å) of $Al_{0.35}Ga_{0.65}As$ ($Al_{0.3}Ga_{0.7}As$) between the 2DHS and the doping layer, of thickness 44 Å(46 Å) and 2D density 9×10^{11}cm^{-2} (8×10^{11}cm^{-2}).

Fig. 1 shows the 0.2 GHz Re(σ_{xx}) vs B for sample 1 at zero backgate bias. For this scan and all other measurements presented in this paper the temperature of the samples was $T \sim 25$ mK. A series of well-developed FQHE conductivity minima can be seen, and Re(σ_{xx}) vanishes again for $B > 10$ T, for the system is well inside the insulating phase. These features are consistent with those of dc magnetoresistance data.

Fig. 2 shows Re(σ_{xx}) vs f traces of sample 1 for several n_s's in $B = 13$ T. On reducing n_s, f_{pk} increases by more than a factor of 3 before Re(σ_{xx}) diminishes to such an extent that the resonant maximum cannot be clearly identified. Decreasing n_s also broadens the peak and reduces its maximal Re(σ_{xx}). The error in reading n_s from the dc transport data is estimated to be $\sim 3\%$ for high n_s and $\sim 10\%$ for low n_s. The small rounded feature at the shoulder of the $n_s = 5.42 \times 10^{10}$cm^{-2} peak is instrumental artefact.

Fig. 3 summarizes parameters of the resonance for the two samples, measured as n_s varies, in fixed B of 13 T. Fig. 3a shows f_{pk} vs n_s from two different cooldowns of each of sample 1 and sample 2. For a given sample f_{pk} varies only 10 percent between cooldowns. Variation between the two samples is much larger, and so is apparently intrinsic to the wafers. In both samples the B dependence of f_{pk}, even at reduced n_s, is much like that observed in ref. [12]: f_{pk} vs B increases, but flattens out at large enough B. By 13 T, f_{pk} vs B is in this flat regime, so that the 13 T f_{pk}, plotted in Fig. 3a, can be regarded as an approximate high B limiting value.

The f_{pk} vs n_s behavior is simpler for sample 2, though the measured range of n_s is less than it was for sample 1. Sample 2 exhibits f_{pk} uniformly decreasing with n_s, with fits of the data to the power law $f_{pk} \propto n_s^{-\gamma}$ that are consistent, given the errors and range of measurement, with $\gamma = 1/2$. Least squares fits, shown on the graph as solid lines, result in $\gamma = 0.46$ and 0.51 for the two different cooldowns of sample 2 (shown as ◯ and □). The f_{pk} vs n_s traces for Sample 1 show three different regions of n_s. In the highest n_s region, ($n_s > 5.0 \times 10^{10}$ cm^{-2}), f_{pk} changes little with n_s. In the intermediate n_s region, ($3.2 \times 10^{10} \leq n_s \leq 5.0 \times 10^{10}$ cm^{-2}), the data can be fit well to $f_{pk} \propto n_s^{-3/2}$, and least squares fits to $f_{pk} \propto n_s^{-\gamma}$ result in the dotted lines shown in the figure, for which $\gamma = 1.66$ and 1.24 for the two cooldowns (shown as ● and ■). In the low n_s region, $1.34 \times 10^{10} < n_s < 3.2 \times 10^{10}$ cm^{-2}, the data on sample 1 are, like all f_{pk} vs n_s for sample 2, consistent with $f_{pk} \propto n_s^{-1/2}$. The least squares fit lines shown in Fig. 3a give $\gamma = 0.58$ for both cooldowns of sample 1 in the low n_s region.

Fig. 3b shows S/f_{pk} vs n_s for the two samples. S is the numerical integral of Re(σ_{xx}) vs f taken over the experimental f range of 0.2 to 6.0 GHz. S is a good measure of the resonance oscillator strength when the tails of the resonance do not extend beyond this f range. S/f_{pk} is plotted in Fig. 3b for comparison with the FL oscillator model [14,15] prediction that $S/f_{pk} = n_s \pi e/B$. While the S/f_{pk} data do appear directly proportional to n_s, the slope of the fit line drawn in the figure, is 0.47 of the FL predicted value, $\pi e/B$. The linearity of S/f_{pk} vs n_s suggests the sum rule can be generalized to a realistic model of the resonance; disagreement with the FL prediction for the slope is expected considering the inconsistency of that model with the observed B dependence of the resonance as reported in ref. [12]. The measured value of the slope is consistent with the resonance oscillator strengths reported earlier [11,12], which are all roughly half of the FL values.

The evolution of the peak as n_s is reduced leads to the definite conclusion that the resonance cannot be modeled as noninteracting individual carriers bound to defects in

the semiconductor host. Fig. 2 shows that as n_s is reduced, Re(σ_{xx}) increases with decreasing n_s in a region of the high f wing of the peak, though the integrated conductivity S decreases. For example, Re(σ_{xx}) at 2.55 GHz increases from 1.2 to 13 μS, on reducing n_s from 5.42 to 3.13 $\times 10^{10}$ cm^{-2}. This means reducing n_s does not only remove oscillators responsible for the resonance, but changes the parameters of these oscillators. This can only happen when the carrier-carrier interaction plays a role in determining f_{pk}.

The data also allow us to rule out "strong pinning" by dilute impurities. In such a model, the pinning potential is strong enough to essentially immobilize carriers bound to impurities, so that rigidly confined domains between impurities oscillate, and the domain size L is independent of the stiffness of the crystal. As n_s is increased, the mass density of the 2D system increases, as does the stiffness of the WC. We maintain that an increase of mass density does not slow down oscillation through inertia for modes with frequency $2\pi f_{pk} \ll \omega_c$. Low frequency ($\omega(q) \ll \omega_c$) modes [17] of the disorder-free classical WC are independent of m^* and hence of mass density; such modes are taken to give the pinning mode frequency when $q \sim 1/L$. Likewise, in high B a harmonic oscillator made up of part of the 2D system has pinning mode frequency ω_- as set down in ref. [14], independent of the oscillator mass density. The case of strong pinning is contrary to what is observed since in that extreme, increasing n_s would increase the WC stiffness and leave L unchanged, and so would increase f_{pk}.

We interpret the increase of f_{pk} with decreasing n_s as a general consequence of weak WC pinning. By definition, in the weak pinning regime, the forces between carriers in the WC are larger than the forces exerted on carriers by impurities, and the Lee-Rice correlation length, or domain size, L, is larger than the WC lattice constant, a. The lattice is crystalline over length L, so the random impurity potential is averaged over area L^2, resulting in the reduction of the effective pinning as L/a increases. Increasing n_s increases WC stiffness and L/a, causing carriers to tend to stay closer to their crystalline positions and to "fall" less into the impurity potential, so that the restoring force and f_{pk} are reduced as L is increased.

The weak pinning theory in Refs. [14] and [15] is a well-developed example of how weak pinning causes f_{pk} to decrease with n_s and even agrees with the $f_{pk} \sim n_s^{-1/2}$ behavior exhibited by much of the data. Following ref. [15], ω_0 is the same as the frequency of a transverse mode of the clean, $B = 0$ WC at wavevector $q = 1/L$: $\omega_0^2 = \mu/n_s m^* L^2$, where μ is the shear modulus of the classical WC, $\mu = \alpha n_s^2 e^2 a/(4\pi\epsilon_0\epsilon) \sim n_s^{3/2}$, and $\alpha \approx 0.02$. The $n_s^{-1/2}$ behavior of ω_0^2 (and hence f_{pk}) is seen on evaluating L by minimizing the total energy, $L \sim \mu a^2/n_i^{1/2} V_0 \sim n_s^{1/2}$, where n_i is the two- dimensional impurity density, and V_0 is the impurity potential strength.

While we conclude that a weak pinning mechanism is needed to explain the observed decrease of f_{pk} with n_s, we know of no theory as yet that can explain all observations on the resonance.The theory of refs. [14,15] gives L/a comparable to unity for observed f_{pk}'s, contrary to the expectation for weak pinning conditions, and also does not explain [12] the B dependence or sharpness at larger n_s of the resonances. By taking into account incommensurate pinning enhancement of the pinning frequency, the work of Ferconi and Vignale [18] gives much larger L/a for the observed f_{pk}. Chitra *et al.* [19] compute conductivity spectra for a weakly pinned WC; the results depend on a number of length scales that characterize the pinned WC. The theory of Fertig [20] predicts the sharpness of the resonances as a consequence of the long-range of the Coulomb interaction, and can address the observed B dependence [11,12] of the resonance. Fertig's theory can also be cast in a weak pinning picture to give $f_{pk} \sim n_s^{-3/2}$, as observed for sample 1 for $5.0 \times 10^{10} > n_s > 3.2 \times 10^{10}$ cm^{-2}.

The observed differences between the two samples must be explained by their different disorder. In these samples, the sources of disorder are remote acceptors, impurities (mainly C acceptors), and heterojunction interface characteristics. By most indications, the disorder of sample 1 is more significant than that of sample 2. In sample 1, smaller spacer and larger doping would increase the influence of remote acceptors, and its mobility and FQHE definition are less than in sample 2. At the same n_s and B, larger disorder would give a larger restoring force in weak pinning, so a larger f_{pk} is expected, consistent with the f_{pk} of sample 1 always exceeding that in sample 2. One possible explanation for the two regimes of decreasing f_{pk} vs n_s in sample 1 would be that more than one type of disorder is playing a role in determining f_{pk}.

In summary, we studied the n_s dependence of the microwave resonance in the high B insulating phase of high quality 2DHS samples, and observed an upward shift in f_{pk} as n_s was reduced. Neither single-particle localization nor an ideal strongly pinned WC could produce such a dependence. When interpreted as the pinning mode of a 2D WC, the data point to weakly pinned WC domains, whose size increases with n_s.

We thank R. Chitra, H. A. Fertig, M. Hilke, D. A. Huse, and P. Platzman for helpful discussions. This work was supported by NSF, and L.W.E. acknowledges support from the state of Florida.

[1] D. C. Tsui, H. L. Stormer, and A. C. Gossard, Phys. Rev.

Lett. **48**, 1559 (1982); R. B. Laughlin, Phy. Rev. Lett. **50**, 1395 (1983).
[2] Y. E. Lozovik and V. I. Yudson, JETP Lett. **22**, 11 (1975); P. K. Lam and S. M. Girvin, Phys. Rev. **B 30**, 473 (1984); D. Levesque, J. J. Weis and A. H. McDonald, Phys. Rev. **B 30**, 1056 (1984).
[3] V. J. Goldman *et al.*, Phys. Rev. Lett. **65**, 2189 (1990).
[4] Y. P. Li *et al.*, Phys. Rev. Lett. **67**, 1630 (1991).
[5] F. I. B. Williams *et al.* in *Localization and Confinement of Electrons in Semiconductors*, Ed. F. Kuchar, H. Heinrich and G. Bauer, (Springer-Verlag, Berlin 1990); E. Y. Andrei *et al.*, Phys. Rev. Lett. **60**, 2765 (1988); and comment by H. L. Stormer and R. L. Willett, *ibid.* **62**, 972 (1989); reply by E. Y. Andrei *et al.*, *ibid.* **62**, 973 (1989).
[6] Y. P. Li *et al.*, Solid State Commun. **95**, 619 (1995).
[7] Y. P. Li *et al.*, Solid State Commun. **96**, 379 (1995); *ibid.* **99**, 255 (1996).
[8] T. A. Kennedy *et al.*, Solid State Commun. **21**, 459 (1977); B. A. Wilson, S. J. Allen, and D. C. Tsui, Phys. Rev. B **24**, 5887 (1981); M. Besson *et al.*, Semicond. Sci. Technol. **7**, 1274 (1992); G. M. Summers *et al.*, Phys. Rev. Lett. **70**, 2150 (1993).
[9] H. Buhmann *et al.*, Phys. Rev. Lett. **66**, 926 (1991); E. M. Goldys *et al.*, Phys. Rev. B **46**, 7957 (1992); I. V. Kukushkin *et al.*, Phys. Rev. B **45** 4532 (1992).
[10] M. A. Paalanen *et al.*, Phys. Rev. B **45**, 11342 (1992); *ibid.* B **45**, 13784 (1992).
[11] L. W. Engel *et al.*, Solid State Commun. **104**, 167 (1997).
[12] C.-C. Li *et al.*, Phys. Rev. Lett. **79**, 1353 (1997).
[13] P. F. Hennigan *et al.*, Physica B **251**, 53 (1998).
[14] H. Fukuyama and P. A. Lee, Phys. Rev. B **17**, 535 (1978); *ibid.* B **18**, 6245 (1978).
[15] B. G. A. Normand, P. B. Littlewood and A. J. Millis, Phys. Rev. B **46**, 3920 (1992); A. J. Millis and P. B. Littlewood, Phys. Rev. **B 50**, 17632 (1994).
[16] M. B. Santos *et al.*, Phys. Rev. Lett. **68**, 1188 (1992).
[17] L. Bonsall and A. A. Maradudin, Phys. Rev. B **15**, 1959 (1977).
[18] M. Ferconi and G. Vignale, Phys. Rev. B **48**, 2831, 1993.
[19] R. Chitra, T. Giamarchi and P. Le Doussal, Phys. Rev. Lett. **80**, 3827 (1998).
[20] H. A. Fertig, cond-mat/9709209. The weak pinning picture is discussed in H. A. Fertig, private communication.

FIGURES

FIG. 1. Real part of 0.2 GHz diagonal conductivity vs magnetic field of sample 1 at $T \sim 25$ mK and zero backgate bias. The inset shows the transmission line on sample surface, with black indicating the evaporated Al film.

FIG. 2. Real part of diagonal conductivity vs frequency of sample 1 at various carrier densities, n_s, in a constant magnetic field of 13 T, $T \sim 25$ mK.

FIG. 3. a. Resonance frequency vs hole density for both sample 1 (● and ■) and sample 2 (shown as ○ and □) in a constant magnetic field of 13 T and $T \sim 25$ mK. Different symbols for the same sample denote different cooldowns. Both solid lines and dotted lines are power law least squares fits to the data. b. Ratio of integrated $\mathrm{Re}(\sigma_{xx})$ over resonance frequency f_{pk}, vs hole density. The solid line is a linear least squares fit to the data.

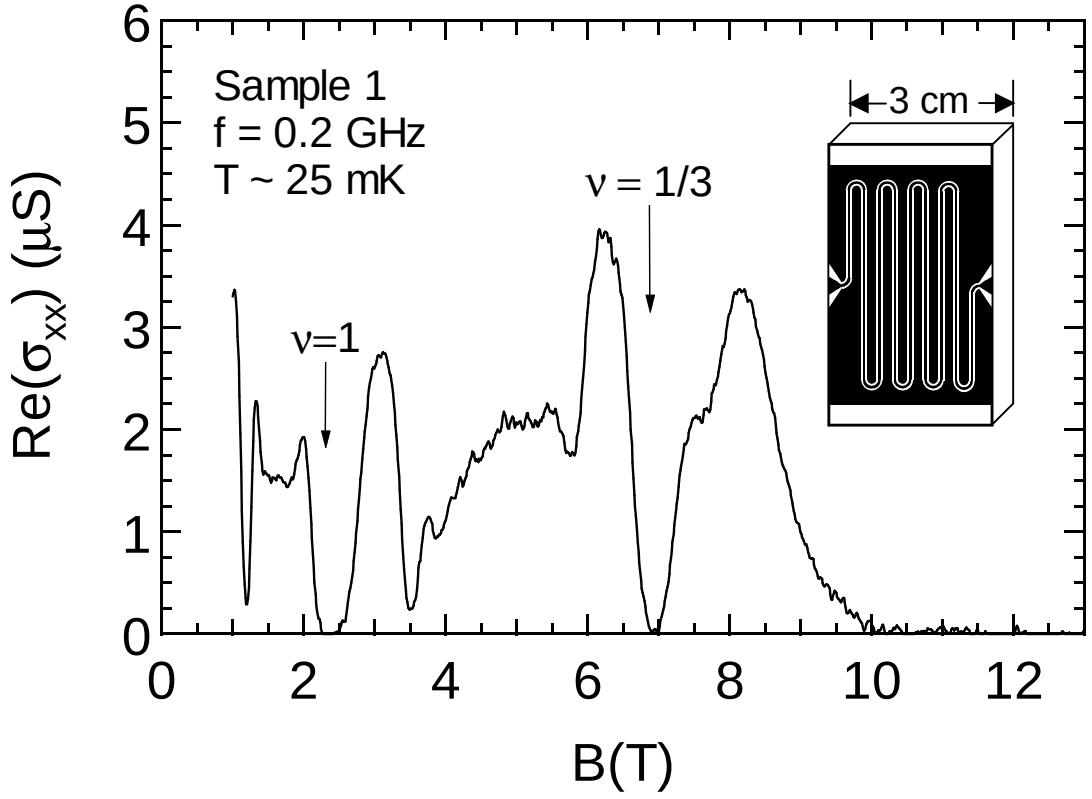

C.-C. Li et al., FIG.1

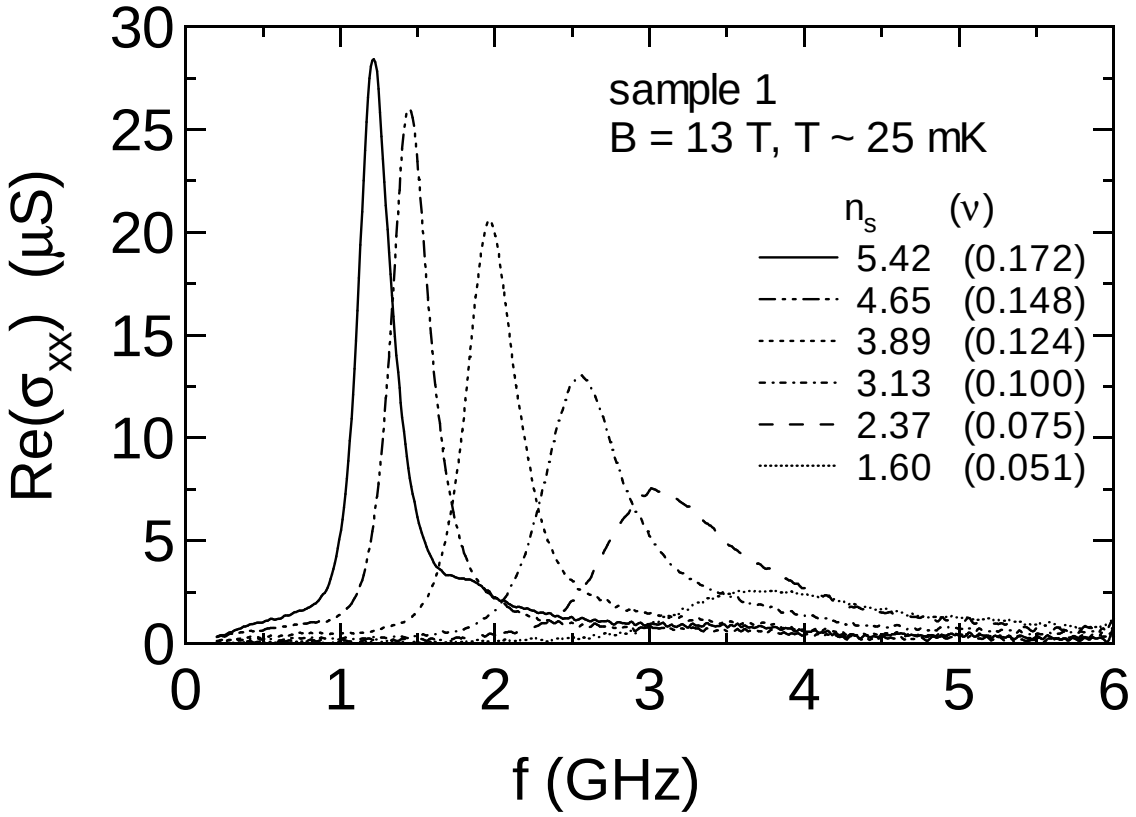

C.-C. Li et al., FIG.2

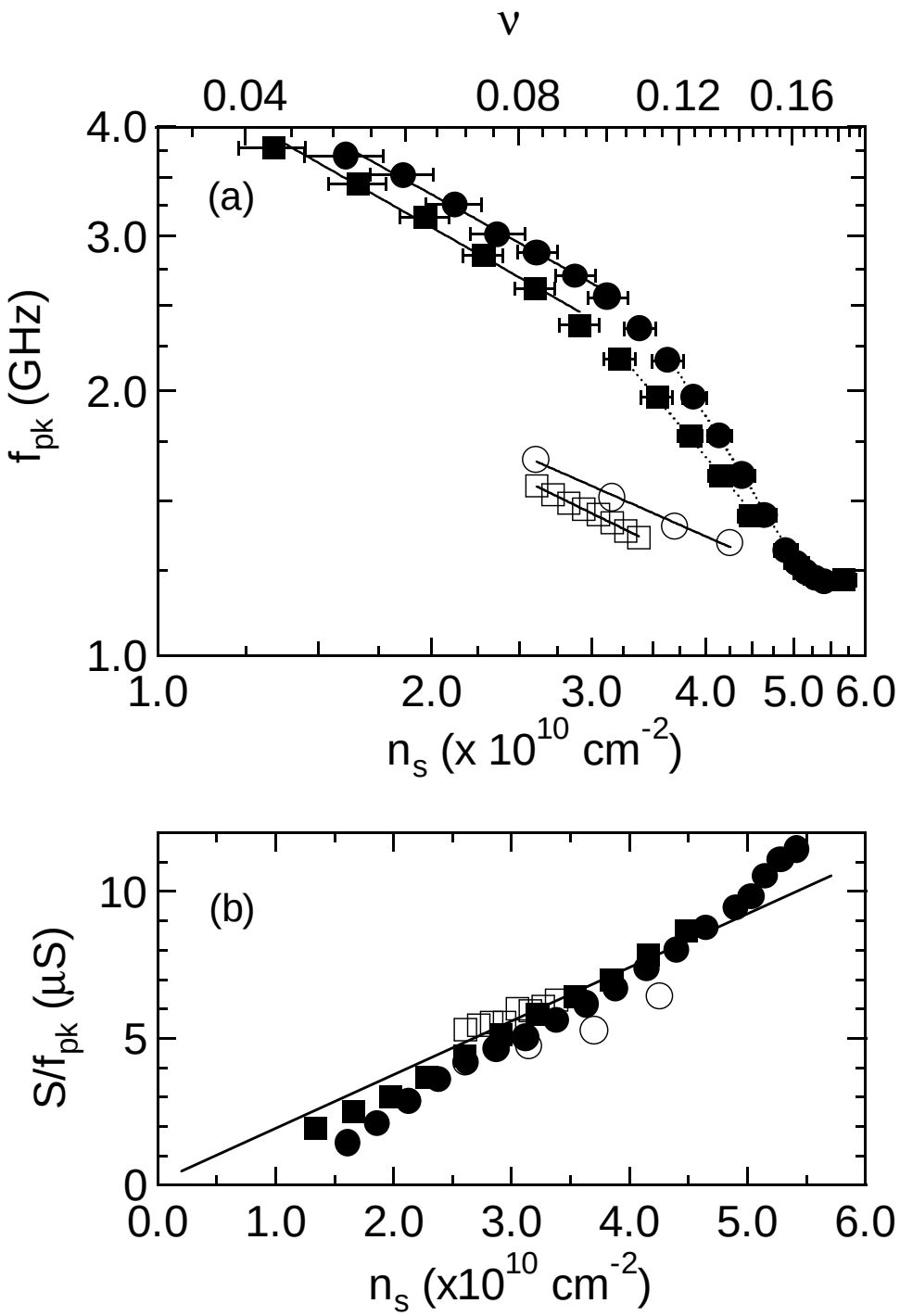

C.-C. Li et al., FIG.3